Penerbit Akademia Baru

Journal of Advanced Research in Fluid Mechanics and Thermal Sciences

Journal homepage: www.akademiabaru.com/arfmts.html
ISSN: 2289-7879

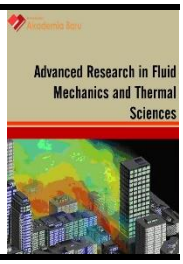

Feasibility Study of Plasma Actuator for Flow Separation Control

Open Access

Md Nizam Dahalan[1,*], Hafizah Zahari[1], Ainullotfi Abdul-Latif[1], Shabudin Mat[1], Shuhaimi Mansor[1], Norazila Othman[1], Mastura Abd Wahid[1], Wan Zaidi Wan Omar[1], Wan Khairuddin Wan Ali[1], Tholudin Mat Lazim[1], Mohd Nazri Nasir[1]

[1] Aeronautics Laboratory, School of Mechanical Engineering, Faculty of Engineering, Universiti Teknologi Malaysia, 81310 Skudai, Johor, Malaysia

ARTICLE INFO

Article history:
Received 6 August 2019
Received in revised form 29 October 2019
Accepted 30 October 2019
Available online 4 February 2020

Keywords:
Plasma actuator; active control; flow separation control

ABSTRACT

The plasma actuator, or dielectric barrier discharged (DBD) actuator, is a flow control technique which comprises three simple components, namely, an exposed electrode, a dielectric layer, and a covered electrode. By providing sufficient applied voltage, the air will locally ionize. In the presence of the electric field, the ionized air induces thrust in the surrounding air, thus jetting the flow in the stream-wise direction, and momentum will be generated in the ambient air, which forms the basis for flow separation control strategy. This project presents the findings of experimental tests and numerical simulations on the operation of plasma actuator under several input conditions and geometries in order to investigate the feasibility of plasma actuator to control the flow separation. An experiment was conducted to visualize the formation of plasma on 0.15 mm thick of Kapton dielectric actuator under an applied voltage of 5 to 10 kVp-p. The results demonstrate that, by increasing the input voltage, the generation of plasma also increases. Moreover, numerical analysis of plasma actuator under various applied voltages, dielectric materials, dielectric thicknesses, and covered electrode widths were computed using COMSOL Multiphysics software. Based on the findings, the trend of the results produced is nearly similar to those of previous researchers. However, further studies are needed to investigate the impact of gas temperature, pressure and flow velocity on the discharge of a plasma actuator.

1. Introduction

The development of flow control technology has become the primary interest of many researchers and engineers in order to increase the aerodynamic characteristics performance of an aircraft by controlling the separation of the flow.

This will typically be achieved when the boundary layer and shear flow on a suction surface are

* *Corresponding author.*
E-mail address: nizam@mail.fkm.utm.my (Md Nizam Dahalan)

manipulated until the separation region is reduced. There are many flow control technologies either passive or active which have been developed, e.g. vortex generators [1-3], Krueger flap [4], Nose-droop technique [5-6], blowing technique using cylinder rotating valve [7], and synthetic jet actuators [8-12]. Active flow control devices serve as a provider of energy used to modify and control the flow separation on surfaces [13]. Even though these technologies are able to improve the maximum lift coefficient, their complexity, heavy weight, volumetric waste and being source of airframe noise and vibration are their weaknesses. Thus, a simple and low-cost technology such as plasma actuator would be a more effective device as an alternative replacement. Plasma actuators have been successfully used in different flow control applications such as exciting boundary layer instabilities on a sharp cone at Mach 3.5 [14], lift augmentation and drag reduction on a swept wing [15], turbulent boundary layer separation control of wing-body configuration [16], and unsteady vortex generation and airfoil leading-edge separation control [17]. Based on previous work, plasma actuators are able to modify the aerodynamic behaviour of an airfoil, by inducing thrust and jetting the flow, consequently delaying the flow separation on the airfoil [17].

The plasma actuator design basically consists of only two electrodes separated by the dielectric layer in between, where the exposed electrode is connected to the high voltage supply, and the covered electrode is grounded. The dielectric layer can be any substance with insulating properties. Commonly used materials are Kapton polymer tape, Teflon tape, Quartz glass, Delrin tape and Macor ceramic. The electrodes are made of copper foil tape. To operate the actuator, a high voltage AC signal is applied to the exposed electrode. This causes a plasma discharge to form over the surface of the dielectric material between the exposed and the covered electrodes. The basic plasma actuator layout shown in Figure 1. When sufficient voltage has been applied, the air will locally ionize in the region of the largest electric field. This occurs at the edge of the exposed electrode. In the presence of the electric field, the ionized air produces a thrust on the ambient air, jetting the flow in the stream-wise direction, hence delaying the separated flow [18]. Momentum transfer thus occurs from charged particles to neutral particles, leading to an electric wind with a maximum velocity of up to 6 m/s [19]. In addition, Shyy *et al.,* [20] who investigated weakly ionized plasma, stated that by adding sufficient amounts of energy to the ionized gas, plasma is formed. The gas is dissociated due to the collisions between those particles whose thermal kinetic energy exceed the molecular binding energy.

The interest to discover the feasibility of plasma actuators in modifying aerodynamic behavior of airfoil has grown in the past few years all around the world. This is due to the special features that include being fully electronic with no moving parts, having a fast time response for unsteady applications, having a very low mass which is especially important in application with high g-loads, being able to apply the actuators onto surfaces without the addition of cavities or holes, having an efficient conversion of the input power into fluid momentum and the easy ability to stimulate their effect in numerical flow solvers [17].

The feasibility of a plasma actuator in controlling the separation was investigated in this project. Two objectives were targeted, the first being to visualize the plasma generated by implementing an experiment on the Kapton dielectric actuator. The intensity of plasma has also been studied under various applied voltages. The second objective is to investigate the thrust induction by plasma actuator under several applied voltages and parameters, including dielectric material, dielectric thickness, and covered electrode width.

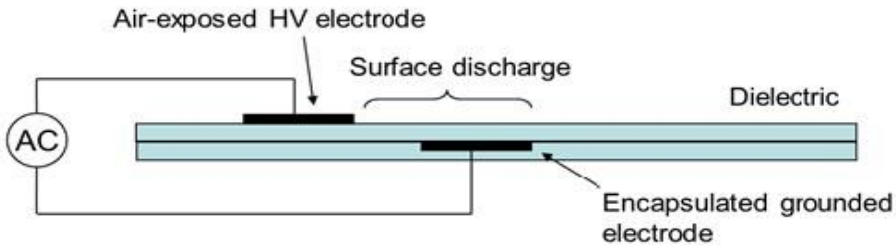

Fig. 1. Plasma actuator layout [19]

2. Methodology

2.1 Experimental Set-up

Figure 2 shows the top view of the plasma actuator mounted on a wooden board, and the side view. The specifications of each of the components of the plasma actuator are given in Table 1. ε is the dielectric constant of the material.

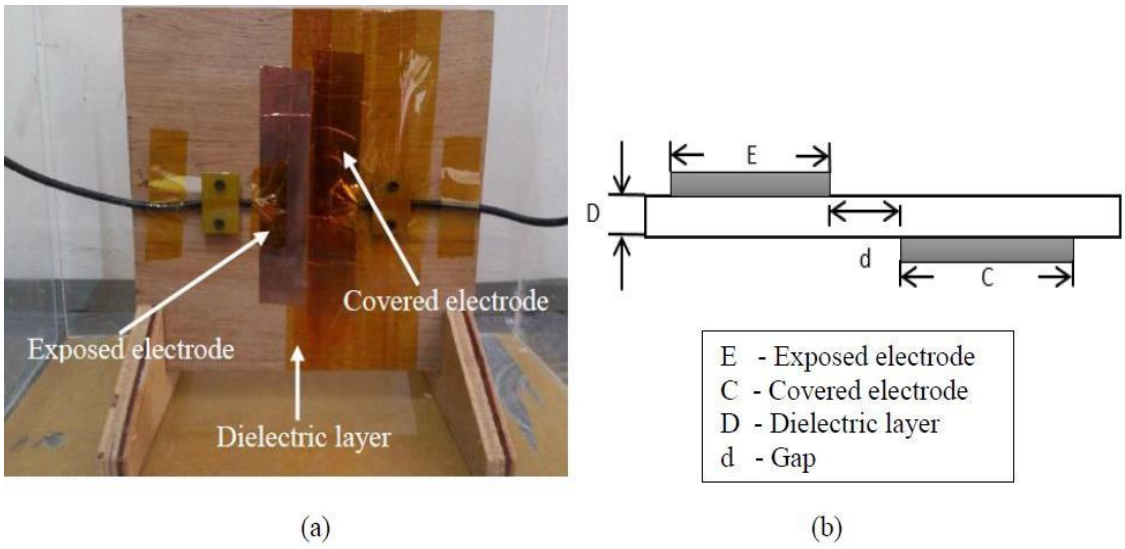

Fig. 2. Design of plasma actuator (a) Top view, as mounted on wooden board (b) Side view

Table 1
Specifications of the plasma actuator design

Component	Material	Condition	Width (mm)	Length (mm)	Thickness (mm)
Exposed electrode, E	Copper	Straight	50	200	0.03
Covered electrode, C	Copper	Straight	50	220	0.03
Dielectric layer, D	Kapton	ε = 3.5	150	250	0.15
Gap, d	-	-	1.0	-	-

Figure 3 shows the schematic diagram of the experimental setup. The actuator consists of two linear electrodes with a thickness of 0.03 mm separated by a Kapton dielectric layer with a 0.15 mm thickness. Both electrodes have a width of 50 mm, and there is 1 mm horizontal displacement between the electrodes. The exposed electrode was supplied with a high voltage in the range of 5 to 10 kVp-p sinusoidal signal form, while the covered electrode was grounded. The intensity of the plasma was recorded and captured using Phantom v710 camera.

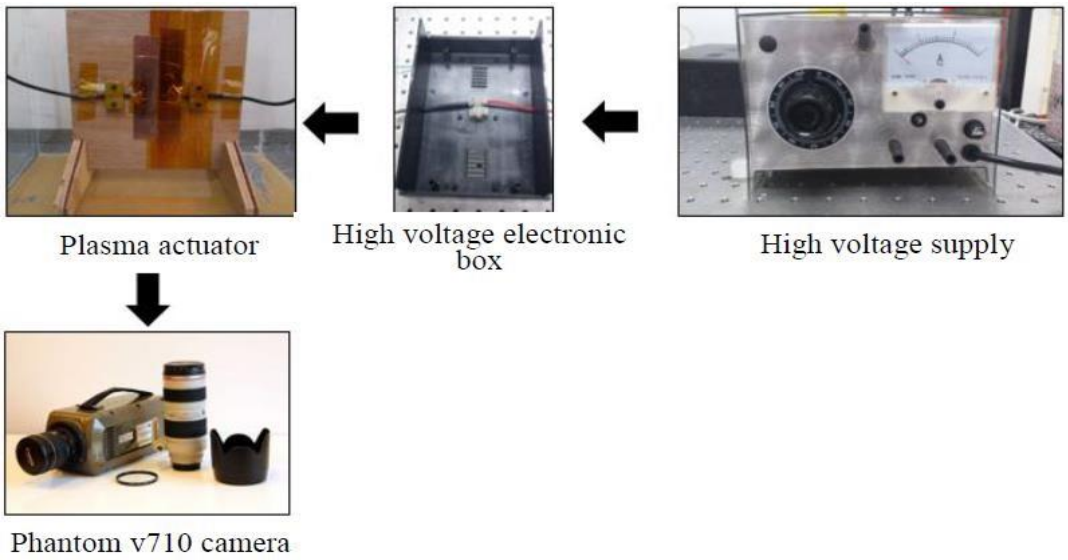

Fig. 3. Schematic diagram of the experimental setup

2.2 Simulation Process

The distribution of electric field and the trend of thrust induced between upper and lower electrodes with a dielectric barrier are numerically computed using COMSOL Multiphysics 4.4 software based on the finite element method (FEM). The formation of the plasma gives rise to an effective thrust on the ambient air. The vector f represents the thrust, produced by the reaction of the electric field with discharged plasma, in Navier-Stokes equations [21].

$$f = \rho_c \boldsymbol{E} \tag{1}$$

where, ρ_c is the net charge density, and $\boldsymbol{E}$ is the electric field. The thrust can be tailored through electrode arrangement, which controls the spatial electric field. The varying strength of the resulting directed momentum of ions to the surrounding air forms the basis for flow control strategies [22].

Furthermore, the trend of induced thrust in charge density of 0.012 C/m^3 was computed under varying applied voltage in the range of 20 to 82 kVp-p. The thrust induced for different dielectric material and thickness was also investigated. The width of the covered electrode varies from 10 to 50 mm. Figure 4 shows the geometry and the discretized mesh of the electrodes and the surrounding region for the computational analysis, focused on the middle region so the reaction of plasma actuator on the edge of the electrode and dielectric layer could be observed and evaluated. The mesh is physics-controlled and extremely fine.

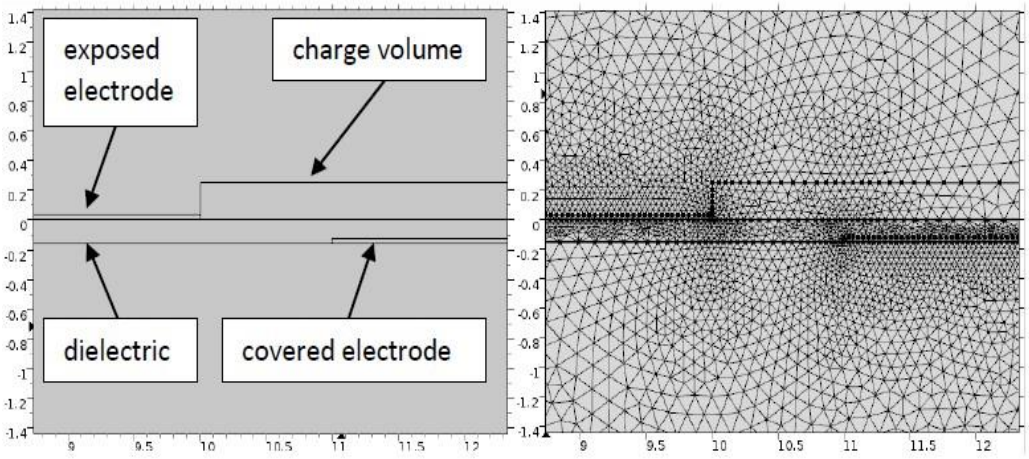

Fig. 4. Drawn geometry and discretized mesh of the computational analysis

A point is randomly observed within the charged volume in order to monitor the induced thrust at variable applied voltages. The coordinates of the point are set as (10.5, 0.115), as shown in Figure 5. The simulation results are then compared with the results obtained from an experiment conducted by Thomas *et al.,* [22].

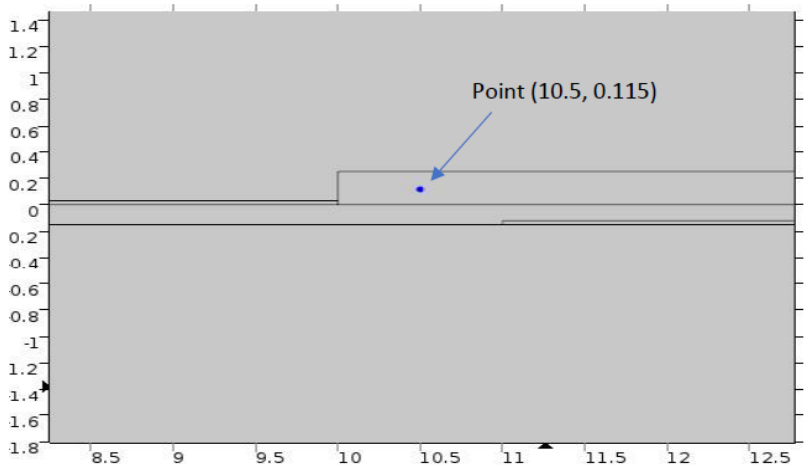

Fig. 5. Point of thrust computation

3. Results and Discussion

3.1 Visual Observation of Plasma Actuator

Figure 6 shows the discharged plasma at 5 to 10 kVp-p applied voltage, with a constant frequency of 20 kHz, captured by a Phantom v710 camera. It can be seen that when the applied voltage was 5 kVp-p, the discharge was relatively diffused. The plasma intensity increased as the applied voltage was increased to 6 kVp-p and 7 kVp-p, but hot spots are not yet observed in the discharge. In contrast, as the applied voltage was increased to 8 kVp-p, some barely-formed hot spots are now seen. When the applied voltage was increased to 9 kVp-p, hot spots formed and are plainly visible. As the applied voltage was increased to10 kVp-p, the number and intensity of the hot spots increased significantly. The results indicate that at low applied voltages, the discharge was in diffused mode, which then becomes highly filamentary at higher voltages. The results obtained are almost similar to the visualization of the plasma actuator operation conducted by Joseph [23].

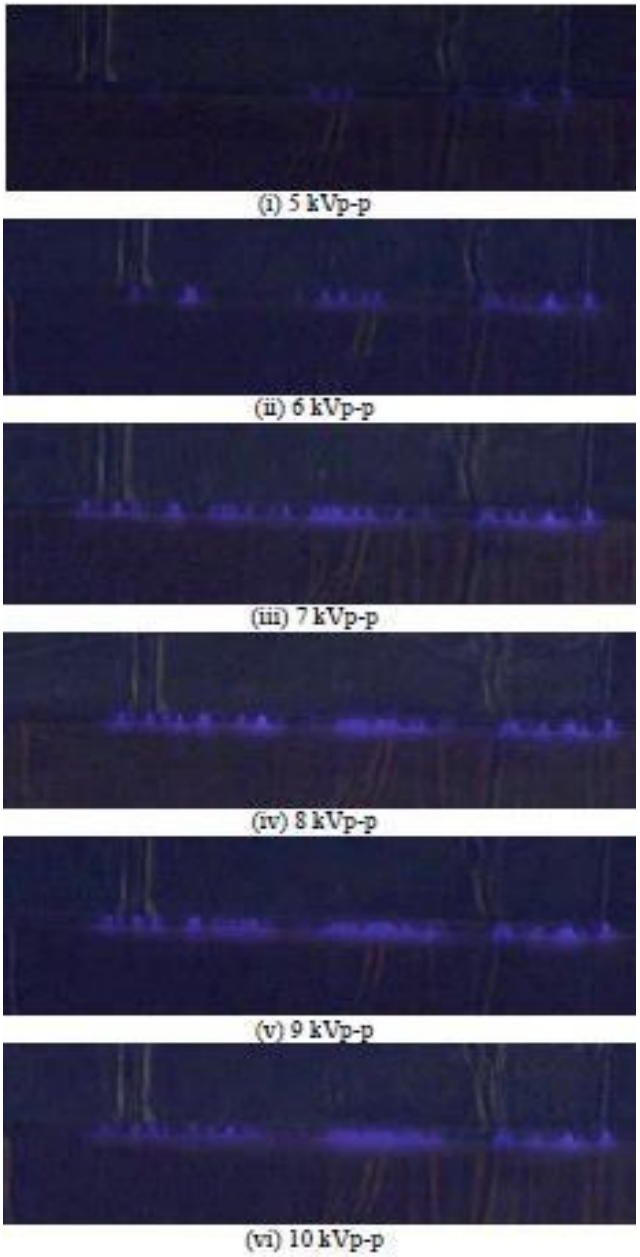

Fig. 6. The plasma discharge at various applied voltage

3.2 Actuator Degradation and Failure

Degradation of an actuator will cause actuator failure. This failure always presents itself as arcing through the dielectric barrier, thus short-circuiting the electrodes. The erosion of the exposed copper electrode is one form of physical actuator degradation [23]. Figure 7 shows the rough or jagged appearance of electrode edge. This occurs after prolonged use; i.e. after approximately four hours of operation, when erosion appeared on the initially smooth surface, next to the plasma formation region.

Figure 7 also shows that the surface of the dielectric proportional to the covered electrode experienced discoloration. This is one physical actuator degradation as well. Initially, the Kapton dielectric had a bright orange-brown colour. After four hours of operation, the dielectric appeared to have a light-coloured opaque discoloration.

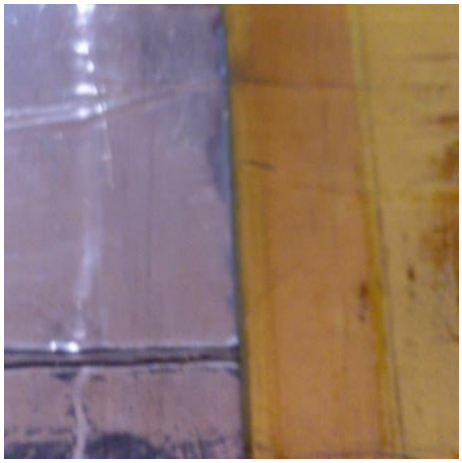

Fig. 7. The electrode erosion and dielectric discoloration

3.3 Induced Thrust of Plasma Actuator

The thrust induced by the plasma actuator is basically obtained from the presence of the electric field. Figure 8 shows the computed electric field and electric potential distribution of the plasma actuator operation region at 5 to 10 kVp-p. The red arrows indicate the vectors of the electric field, while the coloured contour indicate the magnitude of the electric potential.

As discussed in the previous sections, a point was observed within the charged volume to evaluate the induced thrust at various confugurations, including various types of dielectric materials and thickness values, as well as various applied voltages. From Navier-Stokes equations, the force could be calculated by integrating the charge density multiplied by the electric field at a specified point.

3.4 Effects of Applied Voltage

In order to investigate the effects of the input voltage on the plasma actuator, the Teflon dielectric actuator with a constant dielectric thickness of 3.18 mm was used. The actuator was computed with varying applied voltage in the range of 20 to 78 kVp-p. The results obtained show a trend similar to Thomas *et al.*, [22] experimental findings, which are shown in Figure 9. The graph explains that the thrust induced increases as the applied voltage increases. This could be explained by the formation of the electric field, where the higher the applied voltage, the stronger the electric field, which thus induced greater thrust. Note that as the applied voltages become higher, the actuator will experience filamentary mode where degradation will occur, as discussed in the previous section. Other than that, once the actuator experiences filamentary mode, further increase in the applied voltage not only resulted in an insignificant increase in thrust, but significantly increased the dissipated power [22].

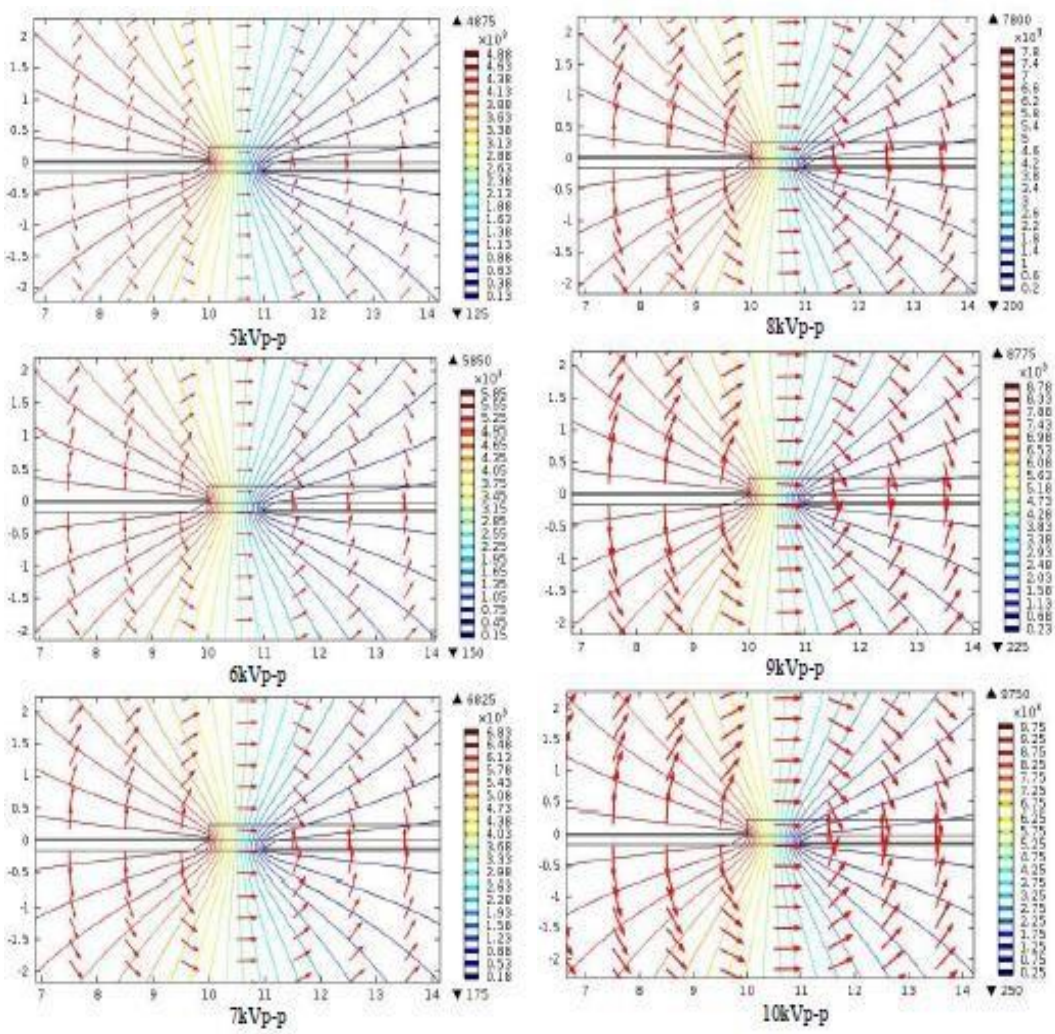

Fig. 8. Computed electric field and electric potential distribution

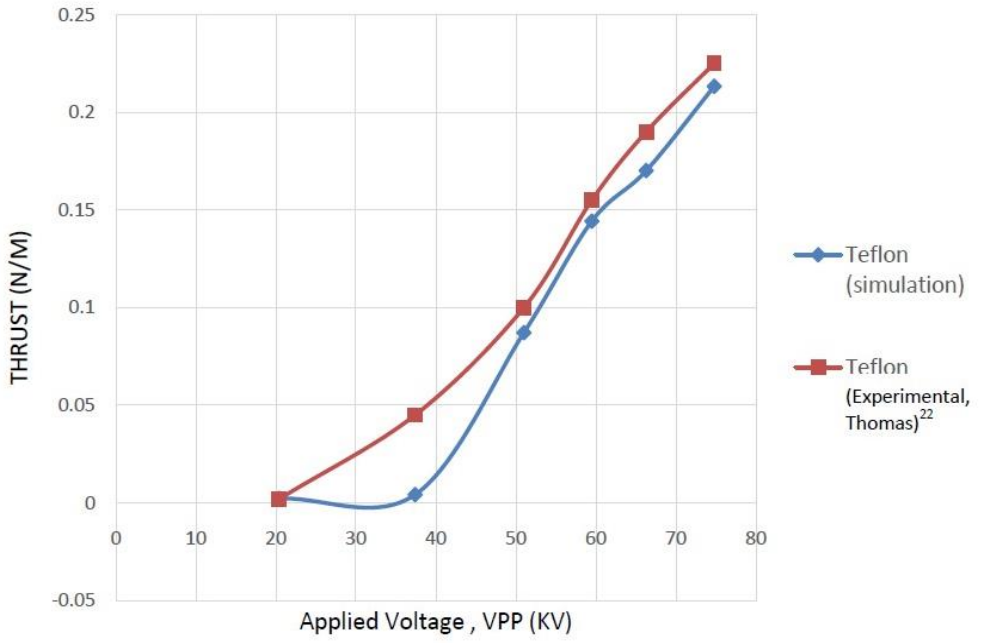

Fig. 9. Computed thrust per unit span for different applied voltage for Teflon (ε = 2, t = 3.18 mm)

3.5 Effect of Dielectric Material

Based on the literature, Kapton Polyimide film was often used as a dielectric barrier in single dielectric barrier discharge (SDBD) plasma actuator [22]. Other materials considered for computational analysis and comparison are Teflon, Quartz, and Delrin. Figure 10 shows the graph of thrust per unit span measured for the plasma actuator using various dielectric materials of 6.35 mm thickness, in the range from 20 to 82 kVp-p.

According to the simulation results, as the input voltage increased from zero to about 82 kVp-p, Teflon dielectric material induced a higher thrust compared to the other dielectric materials. The trend of the thrusts for all dielectric materials appeared to be almost similar to that of the previous researchers [22], indicating reliability in the computational analysis.

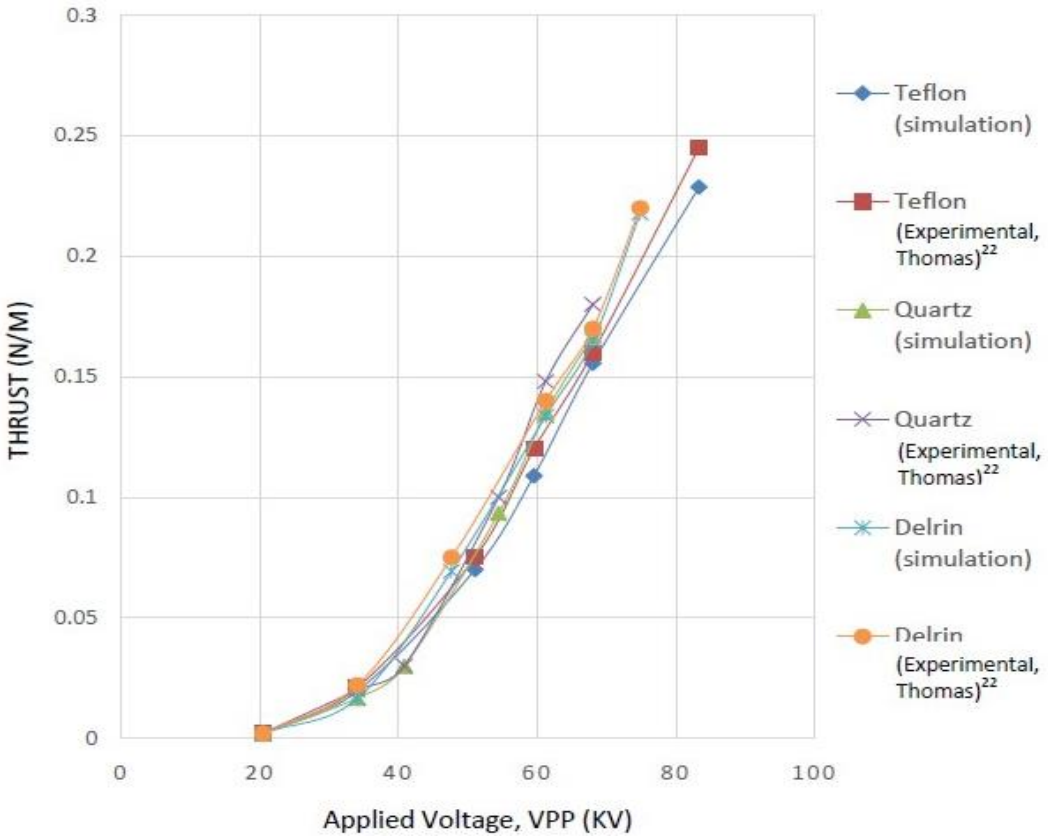

Fig. 10. Computed thrust versus applied voltage for various dielectric materials (t = 6.35 mm)

3.6 Effect of Dielectric Thickness

In another effort to increase the maximum achievable thrust, Teflon was simulated using two different thicknesses, namely 3.18 mm and 6.35 mm. The results are presented in Figure 11. It is clearly seen that variability in thickness significantly affect the thrust. From the graph, although the trend of the thrust as a function of applied voltage for each thickness is the same, it is concluded that the thicker the dielectric material, the smaller is the thrust induced. Numerically, the maximum thrust induced using 3.18 mm and 6.35 mm thick Teflon dielectric actuators are 0.21, and 0.23 N/m respectively. At the lower range of applied voltage, the thinner the electrode, the larger is the thrust induced. However, a thicker dielectric material is able to induce higher thrust in the higher range of input voltage, approximately up to 82 kVp-p [22].

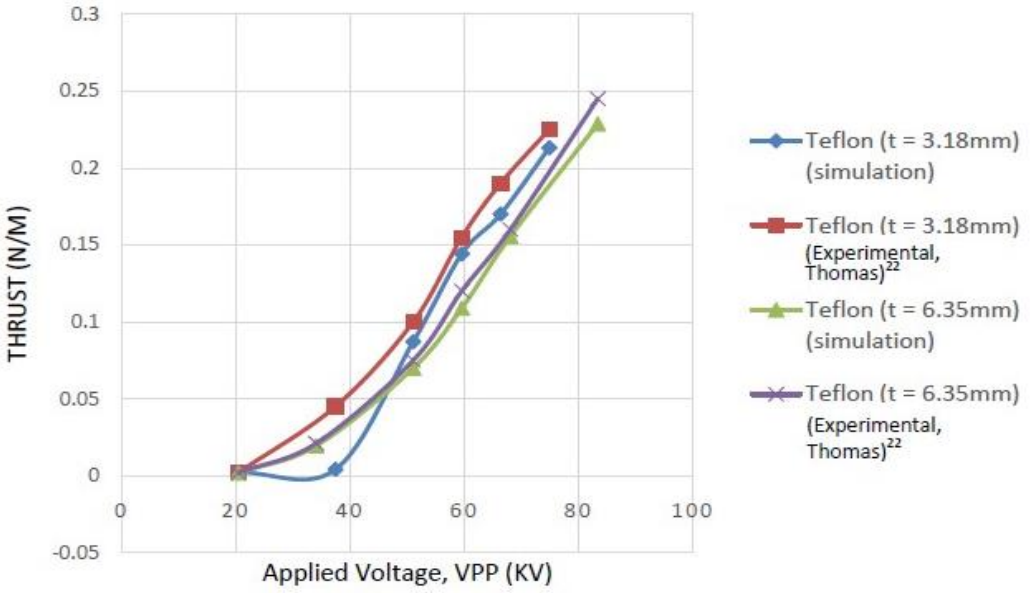

Fig. 11. Computed thrust per unit span versus applied voltage for various thicknesses (ε = 2)

3.7 Effect of Covered Electrode Width

For the next computational analysis, the effect of the width of the covered electrode on the induced thrust was investigated by varying the width within the range from 10 to 50 mm. Figure 12 shows the results for 3.18 mm thick Quartz and dielectric constant of 4.3, at an applied voltage of 20 kVp-p. It can be seen that the induced thrust increases as the width of the covered electrode is increased up to about 35 mm. A further increase in the electrode width does not result in additional thrust. This phenomenon indicates that there is a saturation effect showing that increasing the covered electrode width beyond that necessary to encompass the region of plasma formation does not provide additional thrust benefit [22].

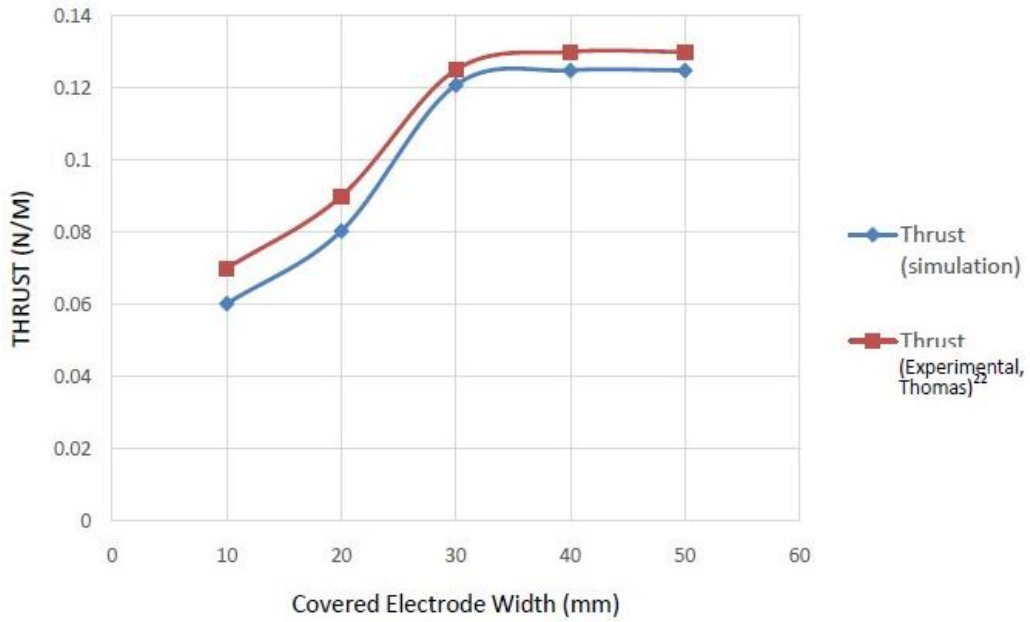

Fig. 12. Computed thrust per unit span versus electrode width for Quartz (ε=4.3, t=3.18 mm)

4. Conclusions

The feasibility of plasma actuator in controlling flow separation was investigated via a series of experiments by visualizing the formation of the plasma and numerical calculations for effective induced thrust in the ambient air. This project demonstrates that the performance of the plasma actuator is dependent upon many different factors, including the actuator applied voltage, electrode geometry, dielectric material, and dielectric thickness. By varying the input condition and geometry of the actuator, the magnitude of induced thrust also varied. The results show that the higher the applied voltage and the thinner the dielectric thickness, the greater the thrust induced. The thrust induced also increased as the width of the covered electrode is increasing until a certain point. The trend of the results is in agreement with the previous research. However, further investigation is needed to investigate the effect of operating frequency and applied voltage waveform, and the impact of gas temperature, pressure and flow velocity on the discharge of a plasma actuator.

Acknowledgement

The authors gratefully acknowledge the support provided by the School of Mechanical Engineering, Faculty of Engineering, Universiti Teknologi Malaysia (UTM). Also, thanks to the UTM Physics Laboratory, Faculty of Science, and UTM Aeronautics Laboratory, School of Mechanical Engineering, for providing the space and equipment for the experiments. This research was funded by a grant from Ministry of Higher Education of Malaysia (FRGS Grant R.J130000.7851.5F051).

References

[1] A. Hamad, Syed Mohammed Aminuddin Aftab, and Kamarul Arifin Ahmad. "Reducing Flow Separation in T-Junction Pipe Using Vortex Generator: CFD Study." *Journal of Advanced Research in Fluid Mechanics and Thermal Sciences* 44, no. 1 (2018): 36-46.

[2] Godard, Gilles, and Michel Stanislas. "Control of a decelerating boundary layer. Part 1: Optimization of passive vortex generators." *Aerospace Science and Technology* 10, no. 3 (2006): 181-191.

[3] Magill, John, Matthew Bachmann, Gregory Rixon, and Keith McManus. "Dynamic stall control using a model-based observer." *Journal of Aircraft* 40, no. 2 (2003): 355-362.

[4] https://www.skybrary.aero/index.php/Krueger_Flaps.

[5] Geissler, W., H. Sobieczky, and M. Trenker. "New rotor airfoil design procedure for unsteady flow control." In *26th European Rotorcraft Forum*, (2000).

[6] Geissler, W., and M. T. Trenker. "Numerical investigation of dynamic stall control by a Nose-Drooping device." *American helicopter society, San Francisco CA* (2002): 23-25.

[7] Lorber, Peter, Duane McCormick, Torger Anderson, Brian Wake, Douglas MacMartin, Michael Pollack, Thomas Corke, and Kenneth Breuer. "Rotorcraft retreating blade stall control." In *Fluids 2000 Conference and Exhibit*, (2000): 2475.

[8] Koopmans E., and Hoeijmakers H.W.M. "Experimental Research on Flow Separation Control Using Synthetic Jet Actuators." In *29th Congress of the International Council of the Aeronautical Sciences (ICAS)*, (2014).

[9] Dahalan, Md Nizam, Shuhaimi Mansor, and Muhammad Muzakkir Faiz Ali. "Study the Orifice Effects of A Synthetic Jet Actuator Design." *Jurnal Teknologi* 77, no. 8 (2015): 1-7.

[10] Zhao, Guoqing, Qijun Zhao, Yunsong Gu, and Xi Chen. "Experimental investigations for parametric effects of dual synthetic jets on delaying stall of a thick airfoil." *Chinese Journal of Aeronautics* 29, no. 2 (2016): 346-357.

[11] Mat, Shabudin B., Mohd Fahmi B. Abdullah, Md Nizam Dahalan, Mazuriah B. Said, Shuhaimi Mansor, Ainullotfi Abdul-Latif, and Tholudin Mat Lazim. "Effects of Synthetic Jet Actuator (SJA) on Flow Topology of Blunt-Edged UTM VFE2 Wing Model." In *55th AIAA Aerospace Sciences Meeting*, (2017): 0326.

[12] Boualem, K., T. Yahiaoui, and A. Azzi. "Numerical Investigation of Improved Aerodynamic Performance of a NACA 0015 Airfoil Using Synthetic Jet." *International Journal of Mechanical, Aerospace, Industrial, Mechatronic and Manufacturing Engineering* 11, no. 3 (2017): 487-491.

[13] Donovan, John, Linda Kral, and Andrew Cary. "Active flow control applied to an airfoil." In *36th AIAA Aerospace Sciences Meeting and Exhibit*, (1998): 210.

[14] Matlis, Eric Hill. "Controlled experiments on instabilities and transition to turbulence on a sharp cone at Mach 3.5." (PhD diss., University of Notre Dame, 2004).
[15] Zhao, Guangyin, Yinghong Li, Hua Liang, Menghu Han, and Yun Wu. "Flow separation control on swept wing with nanosecond pulse driven DBD plasma actuators." *Chinese Journal of Aeronautics* 28, no. 2 (2015): 368-376.
[16] Zhang, Xin, Yong Huang, Xunnian Wang, Wanbo Wang, Kun Tang, and Huaxing Li. "Turbulent boundary layer separation control using plasma actuator at Reynolds number 2000000." *Chinese Journal of Aeronautics* 29, no. 5 (2016): 1237-1246.
[17] Corke, Thomas C., Martiqua L. Post, and Dmitriy M. Orlov. "Single dielectric barrier discharge plasma enhanced aerodynamics: physics, modeling and applications." *Experiments in Fluids* 46, no. 1 (2009): 1-26.
[18] David M. Schatzman, and Flint O. Thomas. "Turbulent Boundary Layer Separation Control Using Plasma Actuators." In *4th Flow Control Conference*, (2008): 1-15.
[19] Moreau, E., Debien, A., Bénard, N., Jukes, T., Whalley, R., Choi, K. S., Berendt, A., Podliński, J., and Mizeraczyk, J. "Surface Dielectric Barrier Discharge Plasma Actuator." *ERCOFTAC Bulletin 94,* (1994).
[20] Shyy, W., B. Jayaraman, and A. Andersson. "Modeling of glow discharge-induced fluid dynamics." *Journal of applied physics* 92, no. 11 (2002): 6434-6443.
[21] Suzen, Yildirim, and George Huang. "Simulations of flow separation control using plasma actuators." In *44th AIAA Aerospace Sciences Meeting and Exhibit*, (2006): 877.
[22] Thomas, Flint O., Thomas C. Corke, Muhammad Iqbal, Alexey Kozlov, and David Schatzman. "Optimization of dielectric barrier discharge plasma actuators for active aerodynamic flow control." *AIAA Journal* 47, no. 9 (2009): 2169-2178.
[23] Joseph W. F. "Thrust Measurement of Dielectric Barrier Discharge Plasma Actuators and Power Requirements for Aerodynamic Control." (Master's thesis, Missouri University of Science and Technology, 2010).